Separation Science and Technology
Publication details, including instructions for authors and subscription information:
http://www.informaworld.com/smpp/title~content=t713708471

Acidichromic Spiropyran-Functionalized Mesoporous Silica: Towards Stimuli-Responsive Metal Ion Separations Media

Christopher T. Burns[a]; Sung Yeun Choi[ab]; Mark L. Dietz[ac]; Millicent A. Firestone[a]
[a] Materials Science Division, Argonne National Laboratory, Argonne, IL, USA [b] Ciba Specialty Chemicals, Tarrytown, NY [c] Department of Chemistry, University of Wisconsin-Milwaukee, Milwaukee, WI, USA

To cite this Article Burns, Christopher T. , Choi, Sung Yeun , Dietz, Mark L. and Firestone, Millicent A.(2008) 'Acidichromic Spiropyran-Functionalized Mesoporous Silica: Towards Stimuli-Responsive Metal Ion Separations Media', Separation Science and Technology, 43: 9, 2503 — 2519
To link to this Article: DOI: 10.1080/01496390802122311
URL: http://dx.doi.org/10.1080/01496390802122311

Separation Science and Technology, 43: 2503–2519, 2008

ISSN: 0149-6395 print/1520-5754 online
DOI: 10.1080/01496390802122311

Taylor & Francis
Taylor & Francis Group

Acidichromic Spiropyran-Functionalized Mesoporous Silica: Towards Stimuli-Responsive Metal Ion Separations Media

Christopher T. Burns,[1] Sung Yeun Choi,[1] Mark L. Dietz,[1] and Millicent A. Firestone[1]
[1]Materials Science Division, Argonne National Laboratory, Argonne, IL, USA

Abstract: An acidichromic silyl spiropyran was synthesized and covalently immobilized on the surface of mesoporous silica (SBA-15) through either post-modification or a co-condensation route. The integration of the spiropyran into the porous silica was probed by thermogravimetric analysis, nitrogen adsorption/desorption studies and UV-Vis optical spectroscopy. While the co-condensation route provides the higher spiropyran loading levels, it also leads to two different states of attachment. Both synthetic procedures favor the formation of the open, merocyanine form of the spiropyran within the framework, but this form can be readily switched from a protonated to a deprotonated state by treatment with buffered aqueous solutions. Preliminary evaluation of the metal ion sorption capabilities of the spiro-functionalized SBA-15 for selected monovalent, divalent, and trivalent metal ions indicates that the spiropyran-modified materials show modestly improved cation exchange characteristics versus the unfunctionalized mesoporous framework.

Keywords: acidichromic, mesoporous silica

INTRODUCTION

For a number of years, there has been considerable interest in the preparation of novel materials for the efficient and selective removal of metal

Received 25 October 2007; accepted 13 March 2008.
Current address for Sung Yeum Choi: Ciba Specialty Chemicals, Tarrytown, NY
Current address for Mark L. Dietz: Department of Chemistry, University of Wisconsin-Milwaukee, Milwaukee, WI, USA.
Address correspondence to Millicent A. Firestone, Materials Science Division, Argonne National Laboratory, 9700 South Cass Avenue, Argonne, IL 60439, USA. Tel.: 630-252-8298; Fax: 630-252-915; E-mail: firestone@anl.gov

ions from various waste streams. Of particular recent interest have been mesoporous silicas, high surface area sorbents characterized by tunable pore size and readily-modified surface chemistry. Although unmodified mesoporous silicas exhibit poor metal ion binding specificity, appropriate organo-functionalization can render them specific for any of a variety of metal ions. Mesoporous silicas surface-modified with thiol ligands, for example, have been shown to exhibit strong Hg, Pt, or Pd binding (1–7). Alternatively, molecularly-imprinted, thiol-functionalized mesoporous silicas have proven useful for Cd^{2+} and Pb^{2+} sorption (8). Similarly, amino-functionalized SBA-15 has been shown to provide strong uptake of Cu^{2+}, Zn^{2+}, Cr^{3+}, and Ni^{2+} (9). More complex functional groups have also been covalently introduced onto mesoporous silica surfaces, including: cyclam moieties, which have been found to complex Eu^{3+} (10); carbamoylphosphonic acids for heavy metals (11); dendrimers, which have been shown to complex Cu^{2+} (12); salicylaldimine complexes for late transition metal ions (13); and acetamide-phosphonate or hydroxypyridinone ligands, which have been demonstrated to exhibit affinity for a variety of radionuclides (14–15).

Concurrent with the growth in interest in mesoporous silicas has been an increasing awareness of the need to incorporate the principles of "green" chemistry into the practice of chemical separations. Among the variety of approaches that might be taken to yield more environmentally benign separations is the reduction in the quantity of reagents consumed in effecting a separation. With this goal in mind, we have begun to seek systems in which the retention of a metal ion on a solid sorbent is controlled by external stimuli such as temperature or light, rather than by a change in the composition of the solution contacting the sorbent. To this end, we report here our preliminary results for the preparation and characterization of a spiropyran–functionalized mesoporous silica. Certain spiropyrans are well known to exhibit metal ion binding properties that vary markedly with exposure (or lack thereof) to UV-visible light of an appropriate wavelength (16). Despite the obvious potential utility of a material combining photocontrol of metal ion binding with high surface area, to date little if any attention has been directed toward the application of spiropyran-functionalized mesoporous silicas (17). In this paper, we describe our initial efforts to incorporate spiropyran moieties into one type of mesoporous silica, SBA-15, via two routes (post-modification and co-condensation), and compare the properties of the materials produced by these approaches.

EXPERIMENTAL

Unless otherwise noted, all reagents were purchased from Sigma-Aldrich (Milwaukee, WI) and were used as received.

- *Synthesis of 6-Iodospiropyran* (***1***). A mixture of 5-iodosalicylaldehyde (4.43 g, 18.1 mmol), 2-methylene-1,3,3-trimethylindoline (3.16 g, 3.22 mL, 18.2 mmol) and ethanol (40 mL) was placed in a 100 mL round bottom flask and heated to reflux. The reaction mixture was stirred at reflux for 4 h, yielding a purple solution and a light colored precipitate. The reaction mixture was allowed to cool to room temperature and reduced in vacuo. Ethanol (20 mL) was added to the light purple residue and a white precipitate was collected by filtration and rinsed with ethanol (2–3 mL). The isolated product was dried overnight in air to yield 6.43 g (88 %) of a white solid. ^{1}H NMR ($CDCl_3$): δ 7.33 (m, 2H), 7.16 (t, $J = 7.7$, 1H), 7.05 (d, $J = 6.9$, 1H), 6.83 (t, $J = 7.5$, 1H), 6.75 (d, $J = 10.3$, 1H), 6.51 (d, $J = 7.8$, 1H), 6.47 (d, $J = 9.1$, 1H), 5.68 (d, $J = 10.3$, 1H), 2.69 (s, 3H), 1.27 (s, 3H), 1.14 (s, 3H). ^{13}C {^{1}H} NMR ($CDCl_3$): δ 154.3, 148.0, 138.2, 136.5, 135.0, 128.2, 127.6, 121.5, 121.2, 120.5, 119.3, 117.4, 106.8, 104.5, 81.4, 51.9, 28.9, 25.8, 20.1. IR: 3057 (sp^2 C-H), 2966 (sp^3 C-H), 1607 (vinyl C=C), 1470 (aromatic C=C), 1256 (asym C-O-C), 1022 cm^{-1} (sym C-O-C).
- *Synthesis of 6-(vinyltriethoxysilyl)spiropyran* (***2***). A mixture of palladium(II) acetate (0.028 g, 0.124 mmol) and tri(ortho-tolyl)phosphine, P(*o*-tolyl)$_3$ (0.075 g, 0.248 mmol) was placed in a 100 mL 2 neck flask under argon purge. Addition of acetonitrile (50 mL) produced a clear yellow solution that was stirred for 20 min under argon. After stirring, **1** (1.00 g, 2.48 mmol) was added to the solution. Triethylamine (1.77 g, 2.41 mL, 17.36 mmol) and vinyltriethoxysilane (0.57 g, 0.63 mL, 2.98 mmol) were added to the suspension via syringe. The reaction mixture was refluxed for 2 h, cooled to room temperature and reduced in vacuo. The product was sequentially treated with a series of solvents (carbon tetrachloride (100 mL), ether (100 mL), and pentane (50 mL)), precipitated solids were removed by filtration and the filtrate reduced in vacuo to yield a tan-colored oil. The product was isolated using Bakerbond NP octadecyl (C_{18}) reverse-phase silica gel using a 99:1 mixture of hexanes: ethyl acetate as the eluent. Fractions were identified by UV-VIS (0.60 g, 52 %). ^{1}H NMR ($CDCl_3$): δ 7.22 (dd, $J = 8.5$, 2.2, 1H), 7.16 (m, 2H), 7.09 (d, $J = 19.3$, 1H), 7.05 (d, $J = 7.2$, 1H), 6.83 (d, $J = 10.2$, 1H), 6.82 (t, $J = 7.5$, 1H), 6.66 (d, $J = 8.4$, 1H), 6.51 (d, $J = 7.7$, 1H), 5.96 (d, $J = 19.3$, 1H), 5.69 (d, $J = 10.2$, 1H), 3.86 (q, $J = 7$, 6H), 2.72 (s, 3H), 1.28 (s, 3H), 1.25 (t, $J = 7$, 9H), 1.15 (s, 3H). ^{13}C {^{1}H} NMR ($CDCl_3$): δ 154.8, 148.5, 148.2, 136.6, 130.0, 129.3, 128.4, 127.6, 125.2, 121.5, 119.8, 119.2, 118.6, 115.1, 114.4, 106.8, 104.6, 58.5, 51.8, 28.9, 25.9, 20.1, 18.3. ^{29}Si NMR ($CDCl_3$): δ - 56.24. IR: 3041 (sp^2 C-H), 2971 (sp^3 C-H), 1608 (vinyl C=C, and C=C-Si), 1485 (aromatic C=C), 1379 (Sp^3 C-H), 1263 (asym C-O-C), 1078 (Si-O), 1022 (sym C-O-C), 803 cm^{-1}

(Si-O-C), 744 cm^{-1} (Si-C). Anal. Calcd for $C_{27}H_{35}NO_4Si$: C, 69.64; H, 7.58; N, 3.01. Found: C, 71.16; H, 7.45; N, 3.19.

- *Post-modification synthesis of SBA-15 with* (**2**). SBA-15 was synthesized according to a procedure reported previously (18). A post-modification procedure was carried out in toluene. Dried, calcined SBA-15 (325 mg) was heated in a toluene solution of **2** (225mg/30ml) at 60°C for 1 h. The purple powder was washed with ethanol using soxhelet extraction for 24 h. A deep violet powder was obtained after drying under vacuum at 50°C for 48 h,. IR: 3745 (SiO-H), 3397 (OH), 2983 (C-H), 1611 (vinyl C=C), 1486 (aromatic C=C), 1395 (Sp^3 C-H), 1080 (Si-O), 960 (Si-OH), 796 (Si-O), 746 cm^{-1} (Si-C).
- *Co-condensation synthesis of TEOS with* (**2**). This material was synthesized under acidic conditions using BASF Pluronic P123 ethyleneoxide/propylene oxide triblock copolymer ($EO_{20}PO_{70}EO_{20}$) as the template. A typical preparation was as follows: 0.282 g of Pluronic P123 was dissolved in a solution consisting of 7.43 mL water and 1.38 mL concentrated HCl at 40°C in a capped 60-mL polypropylene bottle. After complete dissolution of the copolymer, tetraethylorthosilicate (TEOS, 0.51 g, 0.55 mL) was added dropwise and the solution stirred in the capped bottle for 3 h at 40°C. After 3 h of stirring, a solution of **2** (0.20 g) in 2 mL ethanol was added dropwise while stirring at 40°C, producing an orange solution. The bottle was capped and the orange solution was stirred for 20 h at 40°C, then transferred to an oven and kept at 98°C for 24 h. The molar composition of the reaction mixture was TEOS: $EO_{20}PO_{70}EO_{20}$: VTESSp: HCl: $H_2O = 1 : 0.020 : 0.175 : 6.88 : 191$. The formed brown precipitate (0.645 g) was recovered by centrifugation, washed with water, and dried at 25°C. The unreacted copolymer was removed by soxhlet extraction with ethanol for 72 h to yield 0.226 g of brown solid. IR: 3745 (SiO-H), 3397 (OH), 2983 (C-H), 1650 (vinyl C=C), 1486 (aromatic C=C), 1398 (Sp^3 C-H), 1080 (Si-O), 960 (Si-OH), 796 cm^{-1} (Si-O).
- *Metal ion uptake measurements*. The uptake of metal ions by the various sorbents from aqueous solution was measured by equilibration of 1 mL aliquots of tracer-spiked aqueous buffers of appropriate composition (100 mM sodium citrate, pH 2.61; 20 mM sodium acetate, pH 5.50; or 50 mM Tris at pH 6.82 or 8.22) with known weights of the sorbents. Samples were intermittently and vigorously mixed over a 1 h period, and then allowed to stand with occasional mixing overnight permitting adequate time to reach equilibrium. Following centrifugation, the aqueous phase was drawn off and filtered through a syringe equipped with a Luer lock and fitted with a 0.22 μm pore size, 13-mm diameter PVDF membrane filter (Fisher Scientific, Itasca, IL). To avoid loss of radiotracer due to sorption upon vessel walls, all manipulations were performed

using only plastic ware. Counting of samples was performed on a Packard Cobra Autogamma counter.

The extent of radionuclide uptake was expressed in terms of a weight distribution ratio, D_w, defined as follows:

$$D_W = \frac{(A_0 - A_s)/W}{A_s/V}$$

Here, A_0 and A_s represent the aqueous phase activity (cpm) before and after equilibration, respectively; W is the weight of resin (g) and V is the volume of the aqueous phase (mL). The amount of resin used was selected so as to leave a readily measurable activity in the aqueous phase following equilibration. While typically small (2- 20 mg), this amount of resin represents a large excess relative to the amount of radionuclide present.

PHYSICAL METHODS

Unless otherwise indicated, ^{1}H, ^{13}C and ^{29}Si NMR spectra were obtained in $CDCl_3$ using a Bruker Advance DMX-500 spectrometer at ambient probe temperature. ^{1}H and ^{13}C chemical shifts are reported versus $SiMe_4$ and were determined by reference to the residual ^{1}H and ^{13}C solvent peaks. ^{29}Si chemical shifts were referenced to external neat $SiMe_4$. Coupling constants are reported in Hz. Elemental analysis was conducted at Galbraith Laboratories Inc., Knoxville, TN. Transmission FT-IR spectra were obtained using a Bruker Vertex 70 spectrometer equipped with an ATR accessory over the frequency range 4000–650 cm^{-1}. The Spectral resolution was set at 4 cm^{-1} and the signal averaged over 16 scans. Reflectance FT-IR spectra of mesoporous silicas were obtained by placing a small amount of the solid on a gold-coated glass slide and using a Hyperion 7000 Bruker FT-IR microscope over the frequency range 4000–500 cm^{-1}. The spectral resolution was set at 4 cm^{-1} and the signal averaged over 32 scans. Solution and suspension UV-Vis-NIR spectra were recorded from 200 to 1000 nm using a Cary 5 G UV/Vis/NIR spectrophotometer at a spectral resolution of 1 nm. Optical spectra of mesoporous silica materials were also measured in the diffuse reflectance mode using an Ocean Optics fiber-optic coupled CCD spectrometer. Thermogravimetric analysis (TGA) measurements were taken using a TA instrument TGA Q50. Measurements were taken at a heating rate of 10°C/min from 30°C to 600°C under N_2 atmosphere. Nitrogen adsorption/desorption isotherms were measured on a Micrometrics ASAP 2010 Physisorption Analyser. All samples were out-gassed at 23°C under vacuum

overnight. Average pore diameters were calculated using the Barrett-Joyner-Halenda (BJH) method from the adsorption branch of the isotherm (19). The specific surface areas were calculated from the multi-point Brunauer-Emmett-Teller (BET) method starting from a P/P_o of 0.1.

SAXS data were measured using 12 keV X-rays at beamline 12-ID-C at the Advanced Photon Source (APS) at Argonne National Laboratory. Scattered photons were detected by using an area detector, MarCCD (Evanston, IL.), positioned $\sim$2 m from the sample. Standard correction procedures were applied to remove dark current and background from the measured signal. Scattering angles were calibrated using a silver behenate standard. For these measurements, samples were probed as freely suspended powders in tape.

RESULTS AND DISCUSSION

Prior work has examined the impregnation of spiropyran into porous silica via various doping/physisorption strategies (20–23). Here, we examine the chemisorption of spiropyran into a mesoporous silica framework. To promote covalent attachment of the spiropyran to the inorganic framework, a triethoxysilyl-modified spiropyran was synthesized. This functionalized spiropyran, 6-(vinyltriethoxysilyl)spiropyran (**2**), was prepared via the Heck reaction of vinyltriethoxysilane and 6-iodospiropyran, **1**, using the procedure of Yoon and coworkers (Scheme 1) (24).

Integration of the 6-(vinyltriethoxysilyl)spiropyran into the mesoporous silicas was carried out using two procedures (25). The first, a post-modification (“post-mod”) approach, involves grafting the triethoxy groups on the surface silanols of calcined SBA-15 to form stable, robust Si-O-Si linkages. The primary advantage of this method is that the mesoscopic order of the starting silica is guaranteed. The disadvantage,

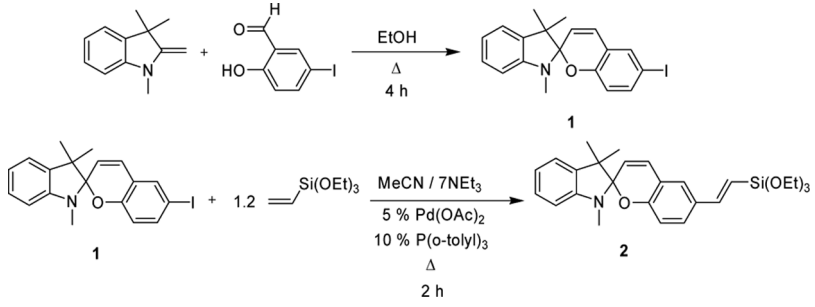

Scheme 1. Synthesis of 6-(vinyltriethoxysilyl)spiropyran

however, is uneven distribution of the grafted organic groups, with functionalization taking place primarily at pore openings (25). The second approach is a co-condensation (''co-cond'') route, involving concurrent formation of the mesoporous silica with a structure directing agent and chemisorption of the 6-(vinyltriethoxysilyl)spiropyran (25). Following formation of the resultant organic-inorganic hybrid silica, the template and unincorporated organosilane are removed by soxhlet extraction. In principle, this direct synthetic route allows for a homogenous distribution of organic groups within the silica channels, but materials prepared by this method frequently suffer from a loss of mesoscopic ordering.

The structures of the spiropyran-functionalized mesoporous silicas prepared using these two synthetic routes, along with that of unfunctionalized, calcined SBA-15, were characterized using SAXS. All of the scattering profiles show four well-resolved Bragg reflections positioned at $1 : \sqrt{3} : 2 : \sqrt{7}$, which are assigned to the (100), (110), (200), and (210) reflections. This is consistent with a well-ordered 2-D hexagonal pore structure. The d_{100} spacing of co-condensed and post-modified spiropyran-functionalized silicas was determined to be 10.55 nm and 10.46 nm, respectively, which compares favorably with that determined for the unmodified SBA-15, 10.46 nm. The corresponding lattice spacing, a, for each of these materials was determined to be 12.18 nm, 12.08 nm and 12.08 nm, respectively.

The morphology of the prepared materials was directly imaged by SEM. All three were found to exhibit tubular morphology, with well-packed 1-D channels (26). From the SEM images, the pore size was estimated to be ca. 5 nm. The pore size distribution and sample surface area were probed by nitrogen adsoption/desorption isotherms and BJH pore-size distribution plots. All samples showed a type-IV isotherm with H1-type hysteresis, which is characteristic of mesoporous solids consisting of cylindrical channels (26). BJH pore-size analyses performed on the adsorption branch showed that all samples have a very narrow pore size distribution. Mean pore sizes of post-mod spiropyran SBA-15 and co-cond spiropyran SBA-15 were 5.0 nm and 4.7 nm respectively, values slightly smaller than that of calcined SBA-15 (5.4 nm). Given that the estimated d-spacings of the three samples were found to be nearly the same (via SAXS analysis), this difference is most likely due to the presence of the spiropyran molecules incorporated into the silica framework. The specific surface area is 630.0 m^2/g for post-mod spiropyran SBA-15 and 576.6 m^2/g for co-cond spiropyran SBA-15, which is also smaller than that of calcined SBA-15 (913.2 m^2/g).

The thermal characteristics of the functionalized silicas were probed via thermogravimetric analysis (TGA), which provides information both on the degradation temperatures of materials and, indirectly, on the level

of inorganic and organic components in the materials. The thermal decomposition of hybrid inorganic-organic materials comprises two general regimes: evolution of absorbed water and gaseous species below 150°C (region I) and evolution of organics from 150°C to 600°C (region II) (27). (The exact products evolved, which obviously depend on the nature of the sample, require identification by mass spectrometry or infrared spectroscopy.) The derivative thermogravimetry (DTG) curves of calcined SBA-15 shown in Fig. 1a are nearly featureless, exhibiting only a rapid initial (below 150°C) weight loss of ca. 3.1 (wt%), presumably due to water. A small secondary weight loss of 0.4 wt % is observed between 150 and 600°C, which may be attributed to residual/absorbed organics. This is compared to SBA-15 from which the organic template has been removed by soxhlet extraction in ethanol in Fig. 1b. Here the DTG curves show not only a more substantial weight loss component below 150°C (14.5 wt. %), but also a broad component between 150

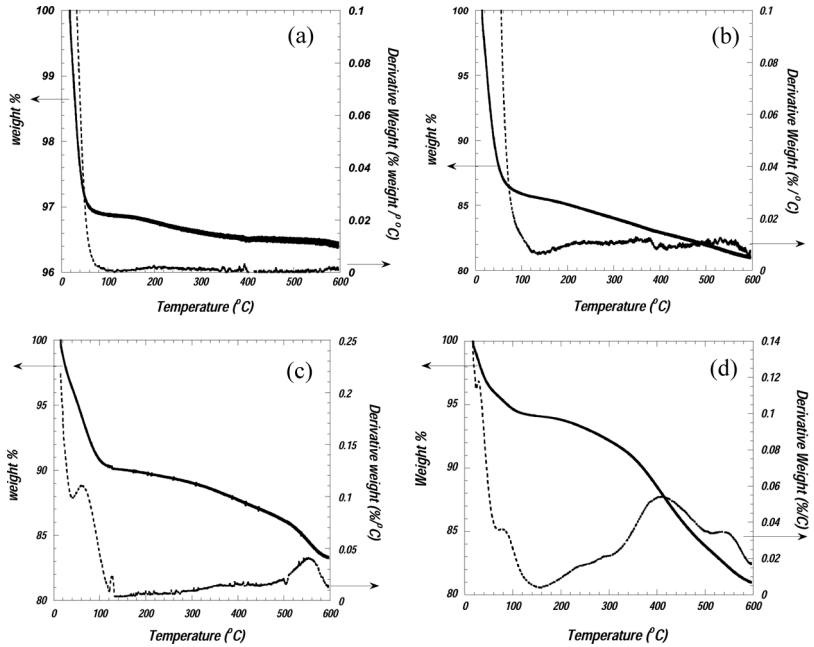

Figure 1. Percentage (solid) and derivative weight loss, DTG, (dashed) curves determined by thermogravimetric analysis (TGA) for (a) calcined SBA-15, (b) ethanol-extracted SBA-15, (c) spiropyran-modified SBA-15 prepared from calcined SBA-15, (d) co-condensed spiropyran-functionalized SBA-15 following template removal by ethanol extraction.

and 600°C, with a total weight loss in this region of 5.5 wt %. Most likely, this is indicative of incomplete removal of the liquid crystalline template. In the case of materials prepared by surface grafting the silylspiropyran onto calcined SBA-15 (Fig. 1c), an initial weight loss below 150°C of 9.94 wt. % is observed. Between 150 and 600°C, an additional weight loss of 8.5% is seen, which is attributed to spiropyran incorporated into the framework. The TGA profile collected on the hybrid material prepared by co-condensation of the spiropyran (Fig. 1d) displays the most complicated weight loss profile, exhibiting the expected initial fast loss below 150°C (5.7 wt. %), a second component between 150°C–320°C (2.3 wt. %), a third component between 320°C and 500°C (8.4 wt. %), and a final component between 500°C and 600°C (2.4 3wt. %). The highest temperature component compares well with that observed in the post-modified material, suggesting the presence of the same type of organic component in both hybrids. The component present between 150°C and 320°C also agrees well with that observed in the post-modified material, as well as the soxhlet extracted sample, and thus, might represent residual liquid-crystalline template. Therefore, the large component in the co-condensed system between 320 and 500°C may correspond to a unique organic component not present in the other systems. That is, this difference can be interpreted to mean that co-cond spiropyran SBA-15 has two different chemisorbed organic species within the pores, while post-mod spiropyran SBA-15 has only one.

The integrity and state of the chemisorbed spiropyran was evaluated by UV-Vis spectroscopy. It is well-established that the optical spectrum of spiropyran is sensitive to its local environment (e. g., pH, temperature and light) (28). Spiropryan in its closed form (''spiro'', SP state) is colorless, while its open, planar merocyanine (MC) state is intensely colored, Fig. 2. Freshly synthesized and dried SBA-15 incorporating spiropyran introduced via the post-modification procedure is a violet powder, while materials prepared via introduction of the spiropyran by the co-condensation method are brown. The diffuse reflectance UV-Vis spectrum of the post-mod spiropyran SBA-15 (Fig. 3a, solid line) shows bands positioned at 570 nm and 390 nm (and a shoulder at 466 nm). These spectral features are consistent with the chemisorbed spiropyran being predominately present in the de-protonated MC (Fig. 2a) form ($\lambda_{max} = 570$ nm) (29–30). The optical spectrum recorded for the co-condensed spiropyran SBA-15 (Fig. 3a, dashed line) features a large absorption band at 448 nm (shoulder at 347 nm) and a smaller peak at 579 nm, consistent with the spiropyran being primarily in the protonated MC (Fig. 2a) state ($\lambda_{max} = 448$ nm) (30–31). The observed difference in the state (protonated vs. deprotonated) of the chemisorbed spiropyran most likely arises from the different synthetic conditions used to chemisorb it

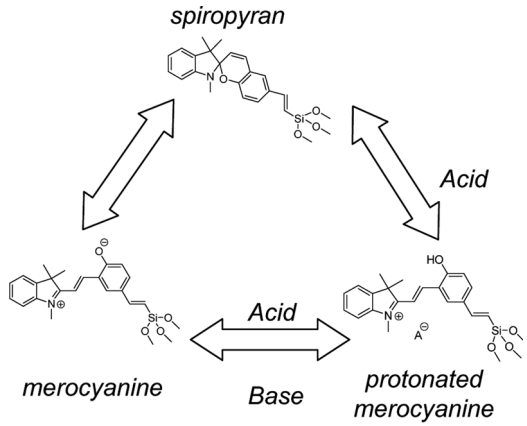

(a)

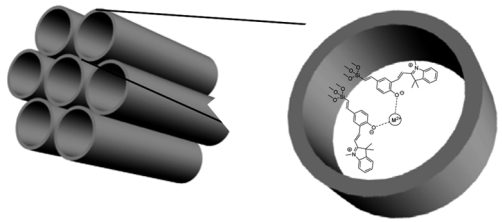

(b)

Figure 2. Schematic illustrations of (a) pH behavior of the silylspiropyran used in this study. (b) Proposed metal complexation by the chemisorbed silylspiropyran.

to the surface of the mesoporous silica. That is, the conditions used to prepare the co-cond spiroypryan SBA-15 are very acidic, while the post-mod spiropyran SBA-15 was prepared under considerably milder, less acidic conditions. Interestingly, these data suggest that the open form is stabilized during the formation of the hybrid material independent of the procedure used to prepare it. The framework-mediated stabilization of the MC state of the chromophore is consistent with prior observations made on spiropyran-doped mesoporous silicas (21).

Although the stabilization of a particular form of the surface-appended chromophore is apparently favored, spiropyrans are well known for susceptibility to interconversion between various states (Fig. 2a). This interconversion was therefore examined by contacting the powders with various aqueous buffer solutions. The acidichromic behavior of the two different materials under acidic (100 mM sodium citrate pH 2.61) and basic (100 mM sodium carbonate, pH 9.35) conditions

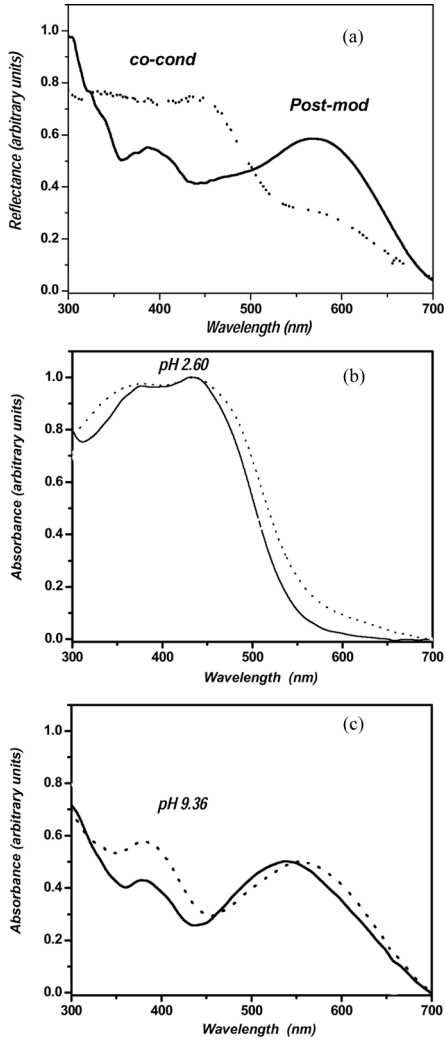

Figure 3. (a) Diffuse reflectance spectra obtained on samples freshly-prepared post-modified spiropyran SBA-15 (solid) and co-condensed spiropyran SBA-15 (dashed) following ethanol extraction of the template. UV-Vis spectra recorded on suspensions of co-condensed (dashed) and post-modified spiropyran (solid) SBA-15 in (b) pH 2.60 citrate buffer and (c) pH 9.36 carbonate buffer.

are presented in Fig. 3b and c, respectively. At low pH (pH 2.60), a suspension of the post-mod spiropyran SBA-15 (solid line, Fig. 3b) shows a UV-Vis spectrum featuring a large peak composed of two components at

435 nm and 376 nm. The co-condensed spiropyran SBA-15 (dashed line, Fig. 3b) displays a similar spectrum with features at 435 nm, 379 nm, and 335 nm. Thus, although the synthetic procedures yield different states of the chemisorbed chromophore, it can be readily converted into the acid state upon contacting with an appropriate buffer solution. Under basic conditions (pH 9.35), the UV-Vis spectrum of the post-mod spiropyran SBA-15 (solid line, Fig. 3c) suspension shows peaks at 540 nm and 378 nm, while that of the co-cond spiropyran SBA-15 (dashed line, Fig. 3c) exhibits features at 560 nm and 378 nm. Nonlinear least squares fitting of the broad peak at 560 reveals that it is actually the superposition of two bands at 567 nm and 648 nm. The shift of the long wavelength peaks to shorter wavelengths in the post-mod derived material (i.e., 540 vs 567 and 648) may signal the presence of aggregated chromophore (20,28). The multiplicity of long wavelength bands observed in the optical spectra between the two variants of the spriopyran-SBA-15 hybrid materials provides additional evidence (in addition to the TGA) that the concondensation route produces two different species of attached chromophore. Future efforts will be directed at the determination of the nature of these two forms. For purposes of this work, however, the most important fact is that the chemisorbed spiropyran, which is primarily in the open, merocyanine state, can be readily interconverted between the protonated and de-protonated states under the acidic or basic conditions.

A second means of assessing the integrity of the chemisorbed spiropyran is by an examination of the metal ion uptake behavior of the spiropyran-functionalized mesoporous silica (Fig. 2b). With this in mind, the sorption of representative monovalent (Na^+), divalent (Ba^{2+} and Co^{2+}), and trivalent (Am^{3+}) metal ions from aqueous solution was evaluated. The results of these determinations, reported as weight distribution ratios, are summarized in Table 1. As is well known, the retention behavior of a metal ion on any given sorbent (i.e., the magnitude of a particular distribution ratio) is a reflection of the strength of interaction of the ion with the various types of surface sites present on the material. SBA-15, like amorphous silica, bears two distinct types of silanol (-Si-OH) sites on its surface (32), which can participate in ion-exchange processes with aqueous phase cations (33). Approximately 20% of these sites, designated as "Q^3 silanols", have a pK_a of *ca.* 2–4.5 (32,34), while the remainder, known as "Q^2 silanols", are significantly less acidic, exhibiting a pK_a of 8.2–8.5 (32,34). The predominance of the latter type of silanols means that unfunctionalized SBA-15, like conventional silica (33,35), is a weak cation-exchanger. Consistent with results obtained previously for conventional silica (33) (on which ions exhibiting the highest charge/radius ratio are most strongly retained, all other things being equal) and a variety of other organic and inorganic ion-exchange

Table 1. Metal ion uptake from aqueous solution by mesoporous silicas

Metal ion	Aqueous phase pH	D_w SBA-15	D_w Post-modified spiropyran SBA-15	D_w Co-condensed spiropyran SBA-15
Am^{3+}	2.61	1,610	2,240	2,350
	5.50	3,020	–	–
	6.82	–	–	3,610
	8.22	3,440	7,210	19,000
Co^{2+}	2.61	NM	NM	NM
	5.50	18.7	27.0	16.2
	6.82	33.9	130	214
	8.22	771	1,750	2,600
Ba^{2+}	2.61	48.8	30.3	43.3
	5.50	945	1,240	1,540
	6.82	1,850	3,300	2,680
	8.22	NM	NM	NM
Na^{+}	2.61	NM	NM	NM
	8.22	16.9	9.65	12.5

NM = not measurable; "-" = not measured; $D_w = (A_0–A_s/w)/A_s/V$, where A_0 and A_s are the initial and final concentrations (cpm) of the element of interest in the aqueous phase, w is the weight of sorbent taken (g), and V is the volume of aqueous phase (mL) employed in the uptake experiment. Low values of D_w imply facile stripping, while larger values are indicative of strong metal ion retention.

materials (36,37), retention of the ions of interest on the unmodified mesoporous silica under a given set of conditions (e.g., pH 5.52) follows the order: $Na^{+} < Co^{2+} < Ba^{2+} < Am^{3+}$. Essentially identical results (i.e., weak Na^{+} retention and significantly stronger uptake of Ba^{2+} and Am^{3+}) are obtained for the two functionalized silicas as well, making it difficult to discern from these data the precise effect of functionalization by spiropyran on the metal ion uptake of the sorbents. The effect is readily apparent, however, from an examination of the results for Co^{2+} sorption. As can be seen from Table 1, under conditions where significant uptake is observed (i.e., pH $\geq$ 6.8), cobalt retention by the unmodified SBA-15 is substantially lower than that of the post-modified material, which in turn, is less than that of the co-condensed material. That the uptake is greater for the co-condensed than for the post-modified material is not unexpected given the higher level of functionalization of the former. The difference in the extent of cobalt uptake is not as great, however, as would be anticipated from the difference in functionalization levels, a possible consequence of the fact that when functional groups are introduced by co-condensation of a functional silane, they can be either

present in micropores or hidden in the silica matrix and thus, not readily accessible (32). That either approach to derivatization yields a material exhibiting uptake greater than that of unmodified SBA-15 indicates that Co^{2+} has a greater affinity for a bound spiropryan than for a silanol group. This observation is consistent with results obtained by Byrne et al.,(16) who in the course of efforts to devise optical sensors based on spiropyran-derivatized polymers, observed that the merocyanine deprotonated form of the spiropyran, which possess an anionic phenolate site to which cations can bind, is particularly sensitive to cobalt ion. It is interesting to note that to facilitate formation of the requisite 1:2 complex between Co^{2+} and the surface-bound spiropryan, Byrne employed an 8-carbon spacer to tether the spiropyran to the polymer surface, thus providing molecular flexibility sufficient for complexation (16). The results obtained here demonstrate that an alternative to increasing the "reach" of surface-bound spiropyran molecules (via tethering) as a means of facilitating the complexation of cobalt ion (and by analogy, other polyvalent cations) is to significantly increase the level of surface functionalization. It is also interesting to note that the greater cooperativity between bound spiropyran molecules made possible by high levels of matrix functionalization could reasonably be expected to improve the uptake selectivity of the sorbent for divalent cations over monovalent ones. A comparison of the selectivity of the post-modified and co-condensed sorbents for Co^{2+} over Na^{+}, in fact, shows that $\alpha_{Co/Na}$ (the ratio of D_w values for the two ions under a given set of conditions) increases only modestly (from 181 to 208) in going from the post-modified to the co-condensed material. That the results for the two do not differ more substantially may be yet another consequence of the likely inaccessibility of certain of the functional groups in the co-condensed material. Clearly, the precise relationship between metal ion uptake selectivity and the level (and method) of functionalization in these materials is an area warranting further investigation.

Taken together, our results demonstrate that functionalization of mesoporous silica by spiropyran, either through post-synthesis modification of the silica or by direct incorporation of the spiropyran into the silica matrix during its fabrication, can yield an increase in metal ion uptake by the silica. At the same time, the order of uptake observed for unfunctionalized SBA-15 (and conventional silica gel) is preserved for the spiropyran-derivatized materials, a result not unexpected given that modification in this case involves replacement of one type of weak cation-exchange site (a surface silanol group) with another (the phenolate anion of the merocyanine form of spiropyran, Figure 2b). Most importantly, the results indicate that the integrity of the spiropyran is preserved upon chemisorption.

SUMMARY

The results of this study demonstrate that spiropyran moieties can be readily incorporated into mesoporous silica (SBA-15) framework employing either a post-modification of co-condensation approach. The resultant materials exhibit the same well-ordered 2D hexagonal pore structure and high surface area that characterize the unfunctionalized silica. Most important for the purposes of this study are that the integrity of the spiropyran is preserved upon chemisorption and that the open form (merocyanine state) is favored upon incorporation into the mesoporous matrix. These results lay the groundwork for our future efforts in the synthesis of silyl-modified, light activated spiropyrans, which will be directly applicable to the preparation of light-controlled separations media. This work thus provides the basis for the preparation of "next generation" spiropyran-functionalized mesoporous silicas capable of responding to external stimuli. Work addressing this opportunity is now underway in this laboratory

ACKNOWLEDGMENTS

The authors acknowledge the help of Drs. Byeongdu Lee and Sönke Seifert in the SAXS characterization of the mesoporous powders. This work was performed under the auspices of the Office of Basic Energy Sciences, Divisions of Material Sciences, United States Department of Energy, under contract number DE-AC02-06CH11357.

REFERENCES

1. Feng, X.; Fryxell, G. E.; Wang, L. Q.; Kim, A. Y.; Liu, J.; Kemner, K. M. (1997) Functionalized monolayers on ordered mesoporous supports. *Science*, *276* (5314): 923.
2. Liu, J.; Feng, X. D.; Fryxell, G. E.; Wang, L. Q.; Kim, A. Y.; Gong, M. L. (1998) Hybrid mesoporous materials with functionalized monolayers. *Adv. Mater.*, *10* (2): 161.
3. Wu, G.H.; Wang, Z.Q.; Wang, J.; He, C.Y. (2007) Hierarchically imprinted organic-inorganic hybrid sorbent for selective separation of mercury ion from aqueous solution. *Anal. Chim. Acta.*, *582* (2): 304.
4. Billinge, S.J.L.; McKimmy, E.J.; Shatnawi, M.; Kim, H. J.; Petkov, V.; Wermeille, D.; Pinnavaia, T.J. (2005) Mercury binding sites in thiol-functionalized mesostructured silica. *J. Am. Chem. Soc.*, *127* (23): 8492.
5. Etienne, M.; Sayen, S.; Lebeau, B.; Walcarius, A. (2002) Organically-modified mesoporous silica spheres with MCM-41 architecture as sorbents for heavy metals. *Nanoporous Materials*, *141*: 615.

6. Nooney, R.I.; Kalyanaraman, M.; Kennedy, G.; Maginn, E.J. (2001) Heavy metal remediation using functionalized mesoporous silicas with controlled macrostructure. *Langmuir*, *17* (2): 528.
7. Kang, T.; Park, Y.; Yi, J. (2004) Highly selective adsorption of Pt2+ and Pd2+ using thiol-functionalized mesoporous silica. *Ind. Eng. Chem. Res.*, *43* (6): 1478.
8. Fang, G.Z.; Tan, J.; Pan, X.P. (2005) Synthesis and evaluation of an ion-imprinted functionalized sorbent for selective separation of cadmium ion. *Separ. Sci. Technol*, *40* (8): 1597.
9. Liu, A.M.; Hidajat, K.; Kawi, S.; Zhao, D.Y. (2000) A new class of hybrid mesoporous materials with functionalized organic monolayers for selective adsorption of heavy metal ions. *Chem. Comm.*, (13): 1145–1146.
10. Corriu, R.J.P.; Mehdi, A.; Reye, C.; Thieuleux, C.; Frenkel, A. (2004) Preparation of ordered SBA-15 mesoporous silica containing chelating groups. Study of the complexation of Eu-III inside the pore channels of the materials. *New J. Chem.*, *28* (1): 156.
11. Yantasee, W.; Lin, Y.H.; Fryxell, G.E., Busche, B.J.; Birnbaum, J.C. (2003) Removal of heavy metals from aqueous solution using novel nanoengineered sorbents: Self-assembled carbamoylphosphonic acids on mesoporous silica. *Separ. Sci. Technol.*, *38* (15): 3809.
12. Yoo, S.; Lunn, J.D.; Gonzalez, S.; Ristich, J.E.; Simanek, E.E.; Shantz, D.F. (2006) Engineering nanospaces: OMS/dendrimer hybrids possessing controllable chemistry and porosity. *Chem. Mater.*, *18* (13): 2935.
13. Ray, S.; Mapolie, S.F.; Darkwa, J. (2007) Catalytic hydroxylation of phenol using immobilized late transition metal salicylaldimine complexes. *J. Mol. Catal. a-Chem*, *267* (1–2): 143.
14. Fryxell, G.E.; Lin, Y.H.; Fiskum, S.; Birnbaum, J.C.; Wu, H.; Kemner, K.; Kelly, S. (2005) Actinide sequestration using self-assembled monolayers on mesoporous supports. *Environ. Sci. Technol.*, *39* (5): 1324.
15. Lin, Y.H.; Fiskum, S.K.; Yantasee, W.; Wu, H.; Mattigod, S.V.; Vorpagel, E.; Fryxell, G.E.; Raymond, K.N.; Xu, J.D. (2005) Incorporation of hydroxypyridinone ligands into self-assembled monolayers on mesoporous supports for selective actinide sequestration. *Environ. Sci. Technol.*, *39* (5): 1332.
16. Byrne, R.J.; Stitzel, S.E.; Diamond, D. (2006) Photo-regenerable surface with potential for optical sensing. *J. Mater. Chem.*, *16* (14): 1332.
17. Casasus, R.; Aznar, E.; Marcos, M.D.; Martinez-Manez, R.; Sancenon, F.; Soto, J.; Amoros P. (2007) Photochemical and chemical two-channel control of functional nanogated hybrid architectures. *Adv. Mater.*, *19* (17): 2228.
18. Luan, Z.H.; Fournier, J.A.; Wooten, J.B.; Miser, D.E. (2005) Preparation and characterization of (3-aminopropyl)triethoxysilane-modified mesoporous SBA-15 silica molecular sieves. *Microporous and Mesoporous Materials*, *83* (1–3): 150.
19. Barrett, E.P.; Joyner, L.G.; Halenda, P.P. (1951) The Determination of Pore Volume and Area Distributions in Porous Substances. I. Computations from Nitrogen Isotherms. *J. Am. Chem. Soc.*, *73*: 373.
20. Bae, J.Y.; Jung, J.I.; Bae, B.S. (2004) Photochromism in spiropyran impregnated fluorinated mesoporous organosilicate films. *J. Mater. Res.*, *19* (8): 2503–2509.

21. Schomburg, C.; Wark, M.; Rohlfing, Y.; Schulz-Ekloff, G.; Wohrle, D. (2001) Photochromism of spiropyran in molecular sieve voids: effects of host-guest interaction on isomer status, switching stability and reversibility. *J. Mater. Chem.*, *11* (8): 201.
22. Ariga, K.; Aimiya, T.; Zhang, Q.; Okabe, A.; Niki, M.; Aida, T. (2002) "Proteosilica" a novel nanocomposite with peptide assemblies in silica nanospace: Photoisomerization of spiropyran doped in chiral enviroment. *International J. of Nanoscience*, *1* (5 & 6): 521.
23. Casades, I.; Alvaro, M.; Garcia, H.; Pillani, M.N. (2002) Modified mesoporous MCM-41 as hosts for photochromic spirobenzopyrans. *Photochem. Photobiol. Sci.*, *1* (3): 219–223.
24. Cho, Y.J.; Rho, K.Y.; Keun, S.R.; Kiim, S.H.; Yoon, C.M. (1999) Synthesis of conjugated spiropyran dyes via palladium-catalyzed coupling reaction. *Synth. Commun.*, *29* (12): 2061.
25. Hoffmann, F.; Cornelius, M.; Morell, J.; Froba, M. (2006) Silica-based mesoporous organic-inorganic hybrid materials. *Angew. Chem.-Int. Ed.*, *45* (20): 3216.
26. Gregg, S.J.; Sing, K.S.W. (1967) *Adsorption, Surface Area and Porosity*; Academic Press: London.
27. Xie, W.; Gao, Z.; Pan, W.P.; Hunter, D.; Hunter, Singh, A.; Vaia, R. (2001) Thermal degradation chemisty of alkyl quaternary ammonium montmorillonite. *Chem. Mater.*, *13*: 2979.
28. Minkin, V.I. (2004) Photo-, thermo-, solvato-, and electrochromic spiroheterocyclic compounds. *Chem. Rev.*, *104* (5): 2751.
29. Keum, S.R.; Lee, K.B.; Kazmaier, P.M.; Buncel, E. (1994) A Novel Method for Measurement of the Merocyanine-Spiropyran Interconversion in the Nonactivated 1,3,3-Trimethylspiro-(2h-1-Benzopyran-2,2'-Indoline) Derivatives. *Tet. Lett.*, *35* (7): 1015.
30. Keum, S.R.; Lee, M.J. (1999) Nonactivated arylazoindolinobenzospiropyran derivatives. Part 2: Preparation and kinetic measurements of the spiro-ring formation from the merocyanine form. *Bull. Korean Chem. Soc.*, *20* (12): 1464.
31. Shiozaki, H. (1997) Molecular orbital calculations for acid induced ring opening reaction of spiropyran. *Dyes and Pigments*, *33* (3): 229.
32. Rosenholm, J.M.; Czuryszkiewicz, T.; Kleitz, F.; Rosenholm, J.B.; Linden, M. (2007) On the nature of the bronsted acidic groups on native and functionalized mesoporous siliceous SBA-15 as studied by benzylamine adsorption from solution. *Langmuir*, *23* (8): 4315.
33. Ahrland, S.; Grenthe, I.; Noren, B. (1961) *Acta Chim. Scand.*, *14*: 1059.
34. O'Reilly, J.P.; Butts, C.P.; I'Anson, I.A.; Shaw, A.M. (2005) Interfacial pH at an isolated silica-water surface. *J. Am. Chem. Soc.*, *127* (6): 1632.
35. Krstulovic, A.M.; Brown, P.R. (1982) *Reversed-phase high performance liquid chromatography: Theory, Practice, and Biomedical Applications*; Wiley: New York.
36. Fardy, J.J. (1992) In: *Preconcentration of Trace Elements by Ion Exchangers*, Alfassi, Z.B.; Wai, C.M., eds.; Boca Raton, FL, pp. 181–210.
37. Helfferich, F. (1962) *Ion Exchange*; McGraw-Hill: New York.